Comparative phenotypic analysis of the two major splice isoforms of phosphatidylinositol phosphate kinase type Iγ *in vivo*

Kyle R. Legate[1,*], Dirk Montag[2], Ralph T. Böttcher[1], Seiichiro Takahashi[1] and Reinhard Fässler[1,‡]

[1]Department of Molecular Medicine, Max Planck Institute of Biochemistry, Martinsried, 82152 Germany
[2]Neurogenetics Special Lab, Leibniz Institute for Neurobiology, Magdeburg, 39118 Germany

*Present address: Department of Applied Physics, Ludwig Maximilians University, Munich, 80799 Germany
‡Author for correspondence (faessler@biochem.mpg.de)

Accepted 13 August 2012
Journal of Cell Science 125, 5636–5646

doi: 10.1242/jcs.102145

Summary

Localized production of polyphosphoinositides is critical for their signaling function. To examine the biological relevance of specific pools of phosphatidylinositol 4,5-bisphosphate we compared the consequences of genetically ablating all isoforms of phosphatidylinositol phosphate (PIP) kinase type Iγ (PIPKIγ), encoded by the gene *Pip5k1c*, versus ablation of a specific splice isoform, PIPKIγ_i2, with respect to three reported PIPKIγ functions. Ablation of PIPKIγ_i2 caused a neuron-specific endocytosis defect similar to that found in PIPKIγ$^{-/-}$ mice, while agonist-induced calcium signaling was reduced in PIPKIγ$^{-/-}$ cells, but was not affected in the absence of PIPKIγ_i2. A reported contribution of PIPKIγ to epithelial integrity was not evident in PIPKIγ$^{-/-}$ mice. Given that mice lacking PIPKIγ_i2 live a normal lifespan whereas PIPKIγ$^{-/-}$ mice die shortly after birth, we propose that PIPKIγ-mediated metabotropic calcium signaling may represent an essential function of PIPKIγ, whereas functions specific to the PIPKIγ_i2 splice isoform are not essential for survival.

Key words: PIP kinase, Clathrin-mediated endocytosis, Calcium signalling, Knockout mouse

Introduction

Phospholipid-mediated signaling through phosphatidylinositol (4,5)-bisphosphate [PtdIns(4,5)P_2] regulates a wide variety of cellular functions ranging from gene transcription to actin cytoskeleton remodelling, endocytosis and agonist-induced calcium signaling. To achieve specificity in signaling, the spatiotemporal production of PtdIns(4,5)P_2 must be tightly regulated. PtdIns(4,5)P_2 can be generated by de-phosphorylation of PtdIns(3,4,5)P_3 by 3-phosphatases such as PTEN (phosphatase and tensin homolog deleted on chromosome 10), but more commonly it is synthesized by kinases that phosphorylate PtdIns(4)*P* on the D5 position of the inositol ring [type I phosphatidylinositol phosphate (PIP) kinases] or PtdIns(5)*P* on the D4 position (type II PIP kinases). Since PtdIns(4)*P* is the more abundant phosphoinositide, it is believed that the bulk of PtdIns(4,5)P_2 is synthesized by type I PIP kinases.

Type I PIP kinases comprise a family encoded by three genes, giving rise to PIP kinase type Iα (PIPKIα), PIPKIβ and PIPKIγ (Ishihara et al., 1996; Loijens and Anderson, 1996; Ishihara et al., 1998). The nomenclature for human and mouse PIPKIα and PIPKIβ is switched (i.e. human PIPKIα is mouse PIPKIβ, and vice versa); in this work the mouse nomenclature will be used exclusively. PIPKIs have distinct subcellular localization which likely contributes to their specificity of function (Doughman et al., 2003; Giudici et al., 2006). Furthermore, PIPKIγ is expressed as a variety of different splice variants with distinct subcellular localization patterns (Ishihara et al., 1998; Giudici et al., 2004; Schill and Anderson, 2009; Xia et al., 2011). The two major splice isoforms of PIPKIγ, encoded by the *Pip5k1c* gene in mouse, PIPKIγ_i1 (also known as PIPKIγ635 or PIPKIγ87) and PIPKIγ_i2 (also known as PIPKIγ661 or PIPKIγ90) localize to cell-cell junctions of epithelial cells (Akiyama et al., 2005) or focal adhesions (Di Paolo et al., 2002; Ling et al., 2002), respectively. They differ by the addition of 26 amino acids to the C-terminus of PIPKIγ_i2, that provides a binding site for the clathrin AP-2 adaptor complex β2 and μ subunits, and the integrin adaptor talin (de Pereda et al., 2005; Kahlfeldt et al., 2010).

Overexpression and siRNA knockdown studies have revealed distinct cellular functions for PIPKIγ splice isoforms. Through these approaches it was shown that PIPKIγ_i1 has a specific role in G protein coupled receptor-mediated Ca^{2+} signaling (Wang et al., 2004) and ADP-ribosylation factor 6 (ARF6)-mediated Ca^{2+}-dependent exocytosis (Aikawa and Martin, 2003), whereas PIPKIγ_i2 overexpression or dominant negative expression perturbs focal adhesion formation (Di Paolo et al., 2002; Ling et al., 2002), integrin activation (Calderwood et al., 2004) and adhesion (Powner et al., 2005; Toyofuku et al., 2005). Overexpression studies have also shown that this isoform stimulates clathrin-mediated endocytosis (Bairstow et al., 2006; Krauss et al., 2006; Nakano-Kobayashi et al., 2007) and rear retraction of neutrophils during migration (Lokuta et al., 2007) whereas specific knockdown of PIPKIγ_i2 points to a role for this isoform in E-cadherin trafficking (Ling et al., 2007), chemotactic migration of HeLa cells towards an EGF gradient (Sun et al., 2007) and polarized integrin trafficking through

regulation of the exocyst complex (Thapa et al., 2012). Additional roles in migration, invasion and growth of breast cancer cells (Sun et al., 2010), survival of pancreatic beta cells (Tomas et al., 2010), growth factor-dependent β-catenin transcriptional activity (Schramp et al., 2011) and actin organization at sites of N-cadherin-mediated adhesion (El Sayegh et al., 2007) have been proposed, but splice isoform specificity has not been established.

While *in vitro* approaches have provided valuable insights into the cellular functions of PIPKIs, knockout mouse models and cells derived from these models have addressed biological relevance and cellular function without the potential contribution of siRNA-mediated off target effects or overexpression artifacts. The different phenotypes resulting from genetic disruption of individual PIPKI genes highlights the distinct isoform-specific roles they play in physiology. PIPKIα-deficient mice exhibit increased degranulation of mast cells and an increase in cytokine production leading to anaphylaxis, owing to defects in the cortical actin cytoskeleton (Sasaki et al., 2005). Impaired thrombin-induced IP_3 production in platelets lacking PIPKIβ leads to thrombosis defects in PIPKIβ$^{-/-}$ mice (Wang et al., 2008a), and bone marrow-derived macrophages lacking PIPKIβ are defective in phagocytosis due to reduced actin polymerization in the phagocytic cup (Mao et al., 2009). Whereas both PIPKIα- and PIPKIβ-deficient mice are viable and live into adulthood, PIPKIγ-deficient mice either die at birth with defects in synaptic vesicle trafficking (Di Paolo et al., 2004) or die *in utero* from cardiovascular and neuronal defects (Wang et al., 2007). Simultaneous deletion of PIPKIβ and PIPKIγ worsens the phenotype, with the mice dying in minutes rather than hours, whereas deletion of both PIPKIα and PIPKIγ is lethal during embryogenesis (Volpicelli-Daley et al., 2010). Interestingly, a single allele of PIPKIγ is sufficient for life (Volpicelli-Daley et al., 2010). Cells derived from the perinatal lethal PIPKIγ mice have additionally been used to establish roles for PIPKIγ in vesicle priming in chromaffin cells (Gong et al., 2005), FcγR-mediated phagocytosis (Mao et al., 2009), Ca^{2+} signaling in mast cells (Vasudevan et al., 2009) and adhesion and infiltration of neutrophils (Xu et al., 2010), whereas megakaryocytes derived from the embryonic lethal PIPKIγ mouse have implicated PIPKIγ in mediating attachment of the actin cytoskeleton to the plasma membrane in this cell type (Wang et al., 2008b).

The reason for the striking differences in phenotype of both PIPKIγ knockout mice is not clear. Although western blotting revealed the absence of PIPKIγ protein in lysates derived from both mice, the deletion strategies differ in their details. The perinatal lethal mouse was made by replacing exons 2–6 of PIPKIγ, encoding much of the kinase domain, with a Neo cassette (Di Paolo et al., 2004), whereas the embryonic lethal mouse was made using a β-galactosidase gene trap construct that follows the first exon of PIPKIγ (Wang et al., 2007). Both approaches theoretically result in translation of the first exon (32 amino acids) of PIPKIγ.

We have recently reported that fibroblasts lacking PIPKIγ_i2 have a defect in integrin-mediated adhesion and force coupling (Legate et al., 2011). Here we report a comparison of the phenotypes of mice lacking either all PIPKIγ isoforms (PIPKIγ$^{-/-}$ mouse) or only PIPKIγ_i2 (PIPKIγΔE17 mouse). The PIPKIγΔE17 mouse is viable and fertile. T cells from PIPKIγΔE17 mice show increased LFA-1-mediated adhesion and activation, establishing PIPKIγ_i2 as a negative regulator of T cell activation (Wernimont et al., 2010). Our PIPKIγ$^{-/-}$ mouse was made by targeting the PIPKIγ 3′ UTR for Cre-mediated removal. These mice die shortly after birth with an identical gross phenotype as the mouse model targeting the PIPKIγ kinase domain. However, whereas both PIPKIγΔE17 mice and PIPKIγ$^{-/-}$ mice have a comparable synaptic vesicle endocytosis defect, only cells from the PIPKIγ$^{-/-}$ mouse show defects in metabotropic Ca^{2+} signaling. Therefore, we propose that an essential defect in PIPKIγ$^{-/-}$ mice arises from insufficient intracellular Ca^{2+} signaling in a variety of tissues.

Results

Generation and characterization of PIPKIγ$^{-/-}$ and PIPKIγΔE17 mice

To obtain a conditional deletion of all isoforms of PIPKIγ in mice, we generated embryonic stem (ES) cells in which exon 18 of PIPKIγ, encoding the 3′ UTR, was flanked with LoxP sites (supplementary material Fig. S1A). Since deletion of this region eliminates all polyadenylation consensus sequences, the PIPKIγ mRNA becomes rapidly degraded leading to a loss of protein. In parallel, we generated ES cells in which we flanked exon 17, encoding the talin and AP-2 binding site, with LoxP sites to specifically abolish translation of the PIPKIγ_i2 isoform (Legate et al., 2011). Mutant ES cells were used to generate mouse strains in which the floxed sequences were removed by mating with a transgenic line expressing Cre recombinase. F1 generation pups were screened by Southern blot to confirm germline transmission (supplementary material Fig. S1B). Following Cre-mediated excision of the floxed exons, offspring were genotyped by PCR (supplementary material Fig. S1C). Heterozygous offspring were backcrossed an additional six times into the C57BL/6 background prior to analysis.

To confirm that excision of exon 18 resulted in no detectable PIPKIγ mRNA, RNA was isolated from brain tissue of newborn pups and RT-PCR was performed using primers that anneal to exon 16 and 17, or primers flanking exon 17 to distinguish between PIPKIγ_i1 and PIPKIγ_i2 isoforms. In PIPKIγ$^{-/-}$ mice, no PIPKIγ message was observed, whereas in PIPKIγΔE17 mice the entire message encoding PIPKIγ_i2 had the size of the PIPKIγ_i1 isoform (Fig. 1A). PIPKIγ_i2 was the predominant PIPKIγ isoform in brain, as previously reported (Wenk et al., 2001). The amount of PIPKIα and PIPKIβ transcript was not noticeably changed in the absence of PIPKIγ transcript. Immunoblotting of brain lysates confirmed the complete absence of PIPKIγ protein in PIPKIγ$^{-/-}$ mice, and the absence of PIPKIγ_i2 in PIPKIγΔE17 mice, with all PIPKIγ now migrating as PIPKIγ_i1. The expression levels of talin and clathrin heavy chain were unchanged (Fig. 1B). Likewise, ΔE17 fibroblasts retain expression of PIPKIγ_i1 and express talin at a normal level (Legate et al., 2011).

RT-PCR on tissue samples from wild-type (WT) mice show that expression of both splice isoforms is widespread (supplementary material Fig. S2). Despite the absence of PIPKIγ_i2, PIPKIγΔE17 mice develop normally, are born at normal Mendelian ratios and are indistinguishable from WT littermates in appearance and behavior (Fig. 1C, and data not shown). PIPKIγ$^{-/-}$ mice are born but die a few hours after birth with an apparent inability to feed (note the absence of milk in the stomach; Fig. 1D). There are no histological abnormalities observed in either mouse (data not shown). By comparing these two mice, we conclude that at least one PIPKIγ-specific function

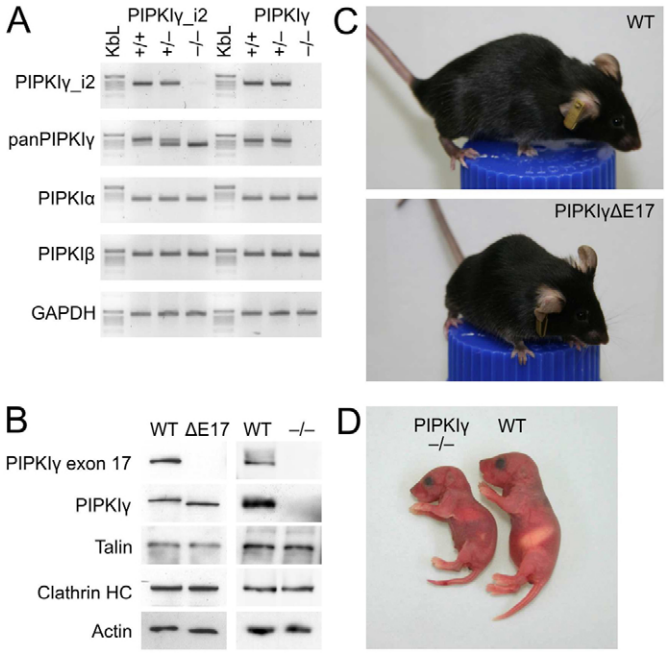

Fig. 1. Generation of PIPKIγ$^{-/-}$ and PIPKIγΔE17 mice. (**A**) RT-PCR from brain cDNA showing the absence of PIPKIγ message in PIPKIγ$^{-/-}$ mice and the specific deletion of PIPKIγ_i2 in PIPKIγΔE17 mice. Expression of PIPKIα and PIPKIβ mRNA is not changed. KbL=Kilobase ladder. (**B**) Western blot of brain lysate shows complete loss of all PIPKIγ isoforms in PIPKIγ$^{-/-}$ mice, using an antibody directed against the kinase domain, and the loss of the PIPKIγ_i2 isoform in PIPKIγΔE17 lysates, using an antibody directed against the C-terminus of PIPKIγ_i2. (**C**) Appearance of 4-week-old WT and PIPKIγΔE17 littermates. (**D**) Appearance of newborn WT and PIPKIγ$^{-/-}$ littermates, at approximately 6 hours *postpartum*. Note the lack of milk in the stomach of the PIPKIγ$^{-/-}$ littermate.

is essential for life, but that PIPKIγ_i2-specific functions are dispensable.

Endocytosis defects in PIPKIγ$^{-/-}$ and PIPKIγΔE17 mice are neuron-specific

The gross phenotype of our PIPKIγ$^{-/-}$ mice resembles that reported by de Camilli and colleagues (Di Paolo et al., 2004). Analysis of these mice revealed a reduction in PtdIns(4,5)P_2 levels in brain accompanied by synaptic vesicle (SV) recycling defects. As PIPKIγ interfaces with the clathrin-endocytosis machinery via interactions between the AP-2 adaptor complex and either the C-terminal extension present in PIPKIγ_i2 (Bairstow et al., 2006; Nakano-Kobayashi et al., 2007; Thieman et al., 2009; Kahlfeldt et al., 2010) or the kinase domain (Krauss et al., 2006) we sought to confirm the findings in our PIPKIγ$^{-/-}$ mouse and extend them to the PIPKIγΔE17 mouse.

To examine SV recycling *in vitro*, neurons were isolated from E14 embryos and SV endocytosis was monitored using a capture ELISA method using synaptotagmin as the specific readout. We did not make note of any obvious migratory defects in neurons during the preparation of this assay, nor were there noticeable neuronal migratory defects *in vivo* (supplementary material Fig. S3 and data not shown). To examine SV endocytosis, surface-biotinylated neurons were first depolarized with 90 mM KCl, and allowed to repolarize in the presence of 4 mM KCl. Neurons from PIPKIγ$^{-/-}$ mice showed around a 50% reduction in synaptotagmin uptake compared to WT neurons, consistent with the reported SV endocytosis defect (Fig. 2A). However, neurons from PIPKIγΔE17 mice also showed a similarly reduced synaptotagmin uptake as PIPKIγ$^{-/-}$ neurons, indicating that the role of PIPKIγ in SV endocytosis is imparted by the C-terminus of PIPKIγ_i2. We confirmed these findings by using a well-characterized FM4-64 fluorescent dye retention assay (Nakano-Kobayashi et al., 2007; Gaffield and Betz, 2007) (supplementary material Fig. S4A). Again, both PIPKIγΔE17 and PIPKIγ$^{-/-}$ neurons showed reduced endocytosis compared to WT neurons (supplementary material Fig. S4B).

Isolation of synaptosomes from WT and PIPKIγΔE17 mice reveals abundant PIPKIγ_i1 in PIPKIγΔE17 synaptosomes (Fig. 2B,C). However, the presence of the PIPKIγ_i1 isoform in the synapse is not able to compensate for the loss of the PIPKIγ_i2 isoform. PIPKIγΔE17 mice performed comparably to WT mice in most standardized behavioral or motor tests (grip strength, rotarod, open field, elevated plus maze, light-dark avoidance, Morris water maze, shuttle box; Fig. 3), the magnitude of the response to an auditory startle stimulus was significantly reduced in PIPKIγΔE17 mice (Fig. 3E,F). The magnitude of response was also decreased at several prepulse intensities, but prepulse inhibition was not affected (Fig. 3F; supplementary material Fig. S5).

To examine whether PIPKIγ has a general role in clathrin-mediated endocytosis in other cell types, we generated kidney fibroblasts from PIPKIγE17 fl/fl and PIPKIγ fl/fl mice and transiently expressed Cre to generate PIPKIγΔE17 and PIPKIγ$^{-/-}$ fibroblasts, respectively (Legate et al., 2011). Transferrin receptor (TfR) endocytosis was then measured in each cell line by monitoring the uptake of Alexa488-transferrin by FACS. Both PIPKIγΔE17 cells (Fig. 2D) and PIPKIγ$^{-/-}$ cells (Fig. 2E) showed the same fluorescence uptake as their WT counterparts, indicating that PIPKIγ plays no obvious role in regulating clathrin-mediated endocytosis in fibroblasts.

To corroborate these findings we investigated spleen-resident metallophilic macrophages (Met-Mφ) that exhibit significant TfR endocytosis *in vivo*. Met-Mφ from WT or PIPKIγΔE17 animals were enriched by magnetic negative selection (Fig. 2F) and then tested for Alexa488-transferrin endocytosis by FACS. Like in fibroblasts, no difference in TfR endocytosis was detected in Met-Mφ from either mouse (Fig. 2G). Likewise, Prussian blue staining of iron stores in spleen sections revealed no differences (Fig. 2H). Finally, challenging mice with a low iron diet caused a significant reduction in iron stores in both spleen and liver, which did not differ between WT and PIPKIγΔE17 littermates (Fig. 2I).

Taken together, a role for PIPKIγ in endocytosis can be readily observed in neurons, but not in other tested cell types. Furthermore, SV endocytosis requires the PIPKIγ_i2 isoform for maximal uptake, but no adverse consequences for survival were apparent by its absence. Therefore, the lethality of PIPKIγ$^{-/-}$ mice arises from impairment of other functions specific to PIPKIγ_i1.

PIPKIγ is not required for epithelial integrity

Knockdown experiments indicate that PIPKIγ is important for basolateral targeting of E-cadherin to adherens junctions (AJs) in MDCK cells (Ling et al., 2007). As defects in epithelial integrity could cause perinatal lethality in PIPKIγ$^{-/-}$ mice, we examined E-cadherin localization in several epithelia. The level and distribution of E-cadherin in AJs in the skin (Fig. 4A), esophagus (Fig. 4B), small intestine (supplementary material

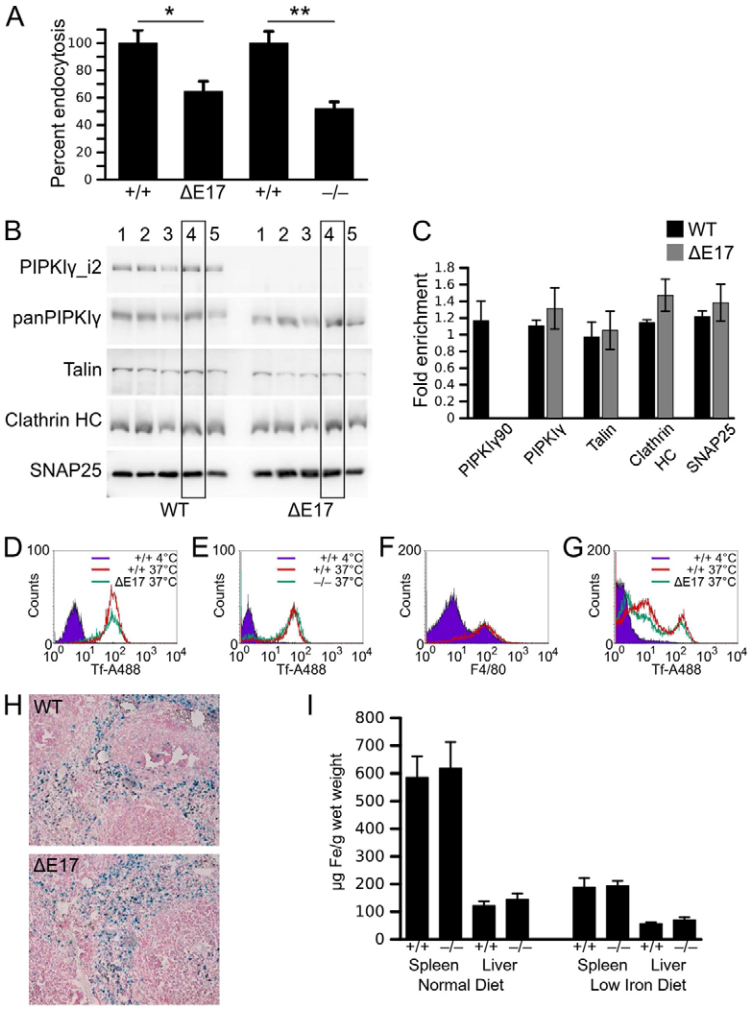

Fig. 2. Analysis of clathrin-mediated endocytosis. (**A**) Neurons from E14 embryos were surface biotinylated, depolarized, and allowed to repolarize for 10 minutes before the amount of internalized synaptotagmin was determined by a capture ELISA assay. WT $n=3$, ΔE17 and $^{-/-}$ $n=4$. $^{*}P<0.05$; $^{**}P<0.005$. (**B**) Brains were isolated from 8-week-old WT and ΔE17 littermates and synaptosomes were isolated on a discontinuous Ficoll gradient. A representative preparation is shown. Lane 1=whole cell lysate; Lane 2=P2 fraction; Lane 3=light membranes; Lane 4=synaptosomes; Lane 5=heavy membranes, mostly mitochondria. The lane containing synaptosomes is bounded by a box. (**C**) Fold-enrichment of the indicated molecules in synaptosomes over whole cell lysate was calculated for six replicates. Data are mean±s.e.m. (**D**) FACS analysis of transferrin (Tf)-Alexa488 endocytosis by WT (red line) and ΔE17 (green line) fibroblasts. A representative example of three independent experiments is shown. (**E**) FACS analysis of Tf-Alexa488 endocytosis by WT (red line) and PIPKIγ$^{-/-}$ (green line) fibroblasts. A representative example of three independent experiments is shown. (**F**) Enrichment of metallophilic macrophages from a WT spleen is shown. Single cell suspensions were labeled with antibody against the macrophage marker F4/80 and analyzed by FACS before (purple area) and after (red line) magnetic negative selection. (**G**) Enriched metallophilic macrophages were incubated with Tf-Alexa488 and endocytosis was monitored by FACS. (**H**) 8 μm thick paraffin-embedded spleen sections were stained with Prussian blue to visualize iron deposits. (**I**) Six animals of each genotype were fed a normal diet or a diet deficient in iron for 6 weeks. Samples of spleen and liver were analyzed for iron storage content. Data are mean±s.e.m.

Fig. S6) and kidney epithelia (Fig. 4C,D) was similar between newborn WT and PIPKIγ$^{-/-}$ mice. Inside-out barrier function of newborn skin was intact, as subcutaneous injection of biotin did not penetrate to the outer layers of epithelia (Fig. 4E). Development of the outside-in barrier was monitored by soaking embryos in a solution of X-gal and monitoring color development due to the presence of endogenous β-galactosidase activity in the dermis. The epidermis was freely permeable in E16.5 embryos, and permeability was restricted to the limbs and face of E17.5 embryos, as previously reported (Hardman et al., 1998) (Fig. 4F). By E18.5, no penetration of X-gal through the epidermis was observed, indicating the complete formation of the outside-in barrier (not shown). To examine whether PIPKIγ localizes to AJs in keratinocytes, and therefore may play a role in AJ formation and maintenance in this cell type, keratinocytes expressing GFP-PIPKIγ_i1 or GFP-PIPKIγ_i2 were differentiated with Ca^{2+} and imaged (Fig. 4G). In contrast to A431 epithelial cells (Akiyama et al., 2005) and MDCK cells (Ling et al., 2007), neither isoform colocalized with E-cadherin in AJs of keratinocytes (Fig. 4G,H). PIPKIγ_i1 localization was largely cytosolic, whereas PIPKIγ_i2 localized to structures resembling focal adhesions at the edge of the cell sheet where cells did not contact neighbors.

Consistent with our finding that PIPKIγ is dispensable for normal epithelial function, conditional knockout mice in which PIPKIγ was deleted from epithelium using Cre recombinase driven by the keratin5 promoter (PIPKIγ fl/fl$^{K5\text{-}Cre}$) were healthy and fertile. Female PIPKIγ fl/fl$^{K5\text{-}cre}$ mice were able to support multiple sequential litters, demonstrating that remodeling of mammary epithelium proceeded normally in the absence of PIPKIγ (not shown).

Agonist-induced Ca^{2+} signaling is reduced in PIPKIγ$^{-/-}$ and enhanced in PIPKIγΔE17mice

A role for PIPKIγ in agonist-induced Ca^{2+} signaling is supported by knockdown and knockout studies in several cell types (Wang et al., 2004; Vasudevan et al., 2009; Yu et al., 2011). To examine whether there are PIPKIγ isoform-specific differences in Ca^{2+} signaling in our mice, we used the ratiometric Fura-2 Ca^{2+} indicator dye to monitor ATP-induced intracellular Ca^{2+} release in WT and PIPKIγ$^{-/-}$ fibroblasts. ATP stimulation triggered a rise in intracellular Ca^{2+} in both cell lines, but the peak response was reduced by 25% in PIPKIγ$^{-/-}$ cells ($P=0.001$) (Fig. 5A,B). Ca^{2+} flux, calculated by measuring the slope of the increase of the Fura-2 fluorescence ratio, was reduced to 70% of wild type values in PIPKIγ$^{-/-}$ cells but this was not statistically significant (Fig. 5B). The lag time between addition of ATP and induction of a response was not different between cell lines (supplementary material Fig. S7A), and all cell lines returned to basal levels of intracellular Ca^{2+} within 5 minutes of stimulation (supplementary material Fig. S7B). Intracellular Ca^{2+} stores were identical between the cell lines as treatment with the SERCA pump inhibitor thapsigargin caused

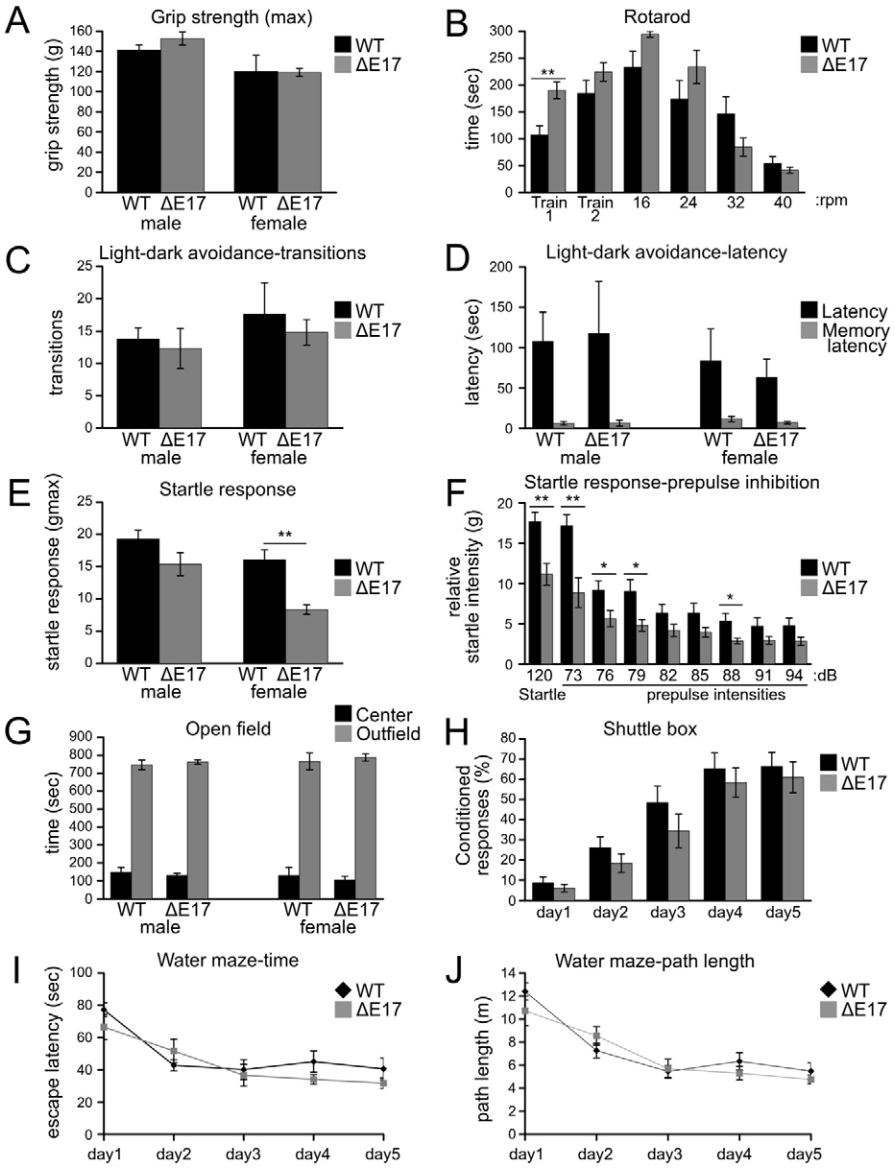

Fig. 3. Behavioral analysis of WT and PIPKIγΔE17 mice. (**A**) Muscle strength was compared by measuring maximum forelimb grip strength. (**B**) Motor coordination was compared by measuring the ability of mice to remain atop a cylinder rotating at the specified revolutions per minute (rpm); training 1 and 2 were executed increasing the rotation continuously from 4 to 40 rpm over 5 min. (**C**) The number of transitions between a light and a dark chamber was used as a measure of anxiety. When tested 18 days later all mice showed a reduced latency time to enter the dark chamber (**D**), indicating an intact long-term memory. (**E**) Startle response resulting from a 120 dB sound. The magnitude of the startle response was significantly lower in ΔE17 mice ($F_{(1,18)}=16.513$, $P=0.0007$). Attenuation of the startle response by a prepulse (**F**) tested sensory gating and information processing. Significant differences in the magnitude of the startle response were observed at prepulse intensities of 73, 76, 79 and 88 dB. The relative inhibition by the prepulse (expressed as % of startle) is not altered (see supplementary material Fig. S4). (**G**) Exploratory behavior in the open field test (center 15×15 cm, outfield area within 5 cm from wall). (**H**) Associative conditioned learning was tested with the shuttle box. (**I**,**J**) The Morris water maze was used to test visual spatial learning. The location of the submerged platform was changed on day 4. Sample sizes for all experiments were 6 WT males, 6 WT females, 4 ΔE17 males and 6 ΔE17 females. *$P<0.05$; **$P<0.005$.

an identical rise in cytoplasmic Ca^{2+} (Fig. 5C). Consistent with the notion that PIPKIγ exerts this affect via phospholipase C (PLC)-mediated hydrolysis of PtdIns(4,5)P_2 to IP_3 and DAG, inhibition of PLC-mediated processes with U-73122 completely abolished the cellular response to ATP (Fig. 5D). Repeating this experiment using PIPKIγΔE17 cells revealed a significantly greater peak response to ATP compared to wild type cells ($P<0.05$) (Fig. 5E,F) with no change in the Ca^{2+} flux. This may be due to the focal adhesion-specific PIPKIγ_i2 isoform contributing to an increased PIPKIγ_i1 level in the absence of exon 17. The lag time between ATP addition and cellular response was not different between WT and PIPKIγΔE17 cells (supplementary material Fig. S7A). The addition of extracellular Ca^{2+} results in a transient increase in the Fura-2 ratio due to store operated Ca^{2+} influx (supplementary material Fig. S7C). The lag time between the addition of extracellular Ca^{2+} was comparable between all cell lines (supplementary material Fig. S7D) but the magnitude of the change in Fura-2 ratio was increased in the absence of either PIPKIγ isoform (Fig. 5G), indicating a greater influx of extracellular Ca^{2+}.

To determine whether the effect of PIPKIγ on Ca^{2+} signaling can be applied to other cell types, astrocytes and bladder-derived smooth muscle cells (SMCs) from WT and PIPKIγ$^{-/-}$ mice were loaded with Fura-2 and exposed to ATP. Like in fibroblasts, PIPKIγ$^{-/-}$ astrocytes showed significantly reduced intracellular Ca^{2+} release than their WT counterparts ($P<0.01$) (supplementary material Fig. S7E). Furthermore, PIPKIγ$^{-/-}$ astrocytes occasionally exhibited an uncoordinated response to ATP exposure, with some cells reacting after a short delay (supplementary material Movie 1), while WT astrocytes responded uniformly to ATP treatment (supplementary material Movie 2). Importantly, ATP-induced Ca^{2+} release did not differ between WT and PIPKIγΔE17 astrocytes (supplementary material Fig. S7E). Exposing SMCs to 100 μM carbachol caused a robust release of intracellular Ca^{2+} stores in WT SMCs, that was significantly reduced ($P<0.0001$) in PIPKIγ$^{-/-}$ SMCs (supplementary material Fig. S7F). Therefore, the absence of PIPKIγ leads to impaired metabotropic Ca^{2+} signaling in several diverse cell types.

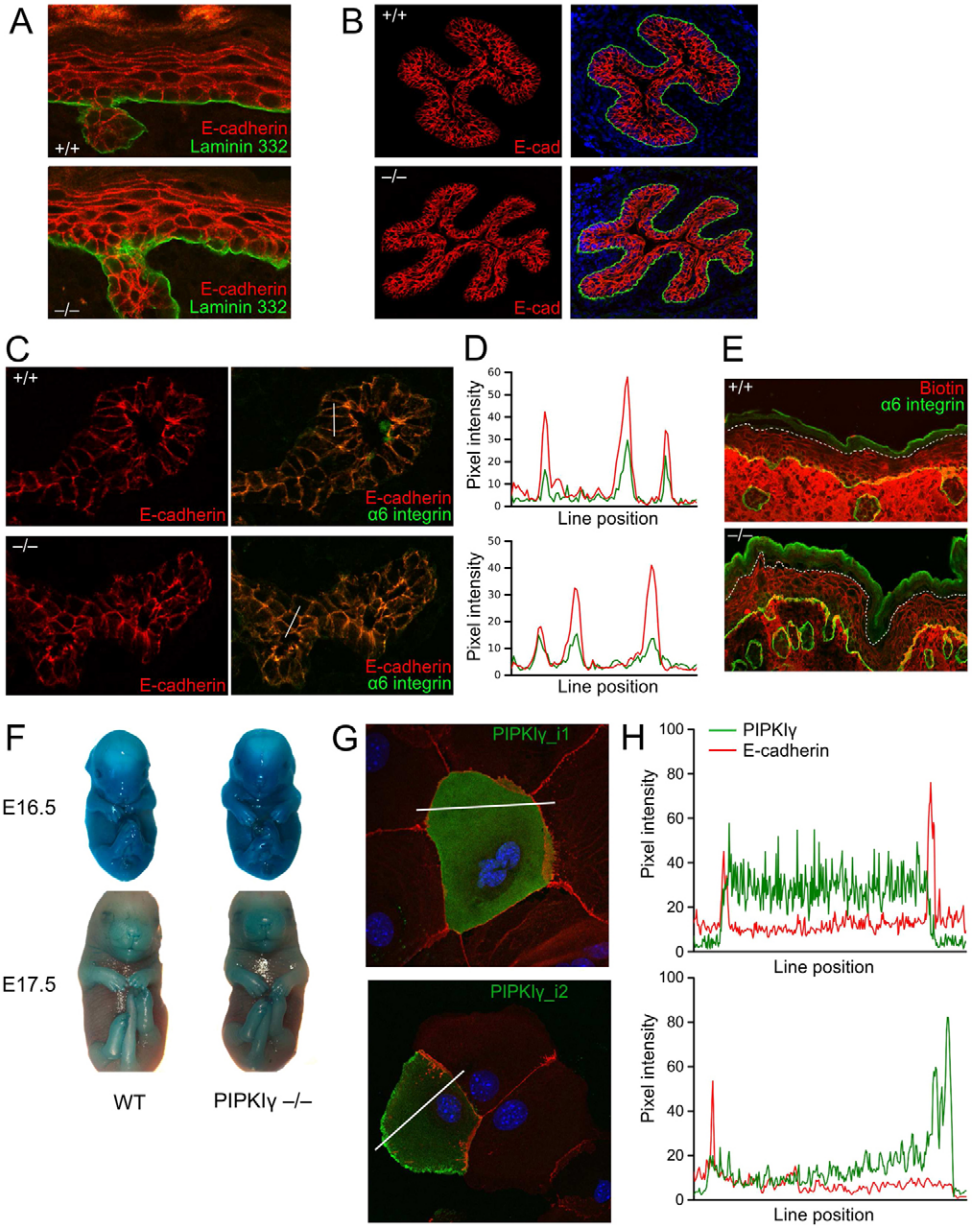

Fig. 4. Analysis of epithelial structure and integrity. (**A**) Sections of newborn back epithelium were immunostained for E-cadherin (red) and Laminin 332 (green) and imaged with confocal microscopy. (**B**) Transverse sections of newborn esophagus were immunostained for E-cadherin (red) and Laminin 332 (green) and imaged with confocal microscopy. (**C**) Sections of newborn kidney were immunostained for E-cadherin (red) and integrin α6 (green). Lines in the merged images denote areas chosen for linescan analysis. (**D**) Linescans from images in C showing coincidence of E-cadherin (red line) and integrin α6 (green line) staining. (**E**) Inside-out barrier function of newborn back skin demonstrated by subcutaneous injection of biotin and detection with streptavidin-Cy3. Note the lack of penetration of biotin into the outer layers of the epidermis (dotted line). (**F**) Outside-in barrier function of the epidermis of E16.5 and E17.5 embryos. Blue color arises from conversion of X-gal by dermal β-galactosidase activity. (**G**) Localization of PIPKIγ isoforms in primary keratinocytes. PIPKIγ$^{-/-}$ keratinocytes were transfected with GFP-PIPKIγ_i1 (top) or PIPKIγ_i2 (bottom), differentiated with Ca^{2+} and immunostained for E-cadherin (red). Lines indicate regions selected for line scan analysis. (**H**) Line scan analysis from regions in G.

Discussion

PtdIns(4,5)P_2 is a lipid messenger with a variety of distinct functions. It can bind directly to many proteins and thereby dictate their subcellular localization and/or functional activity. It is metabolized by phospholipase C to generate the second messengers diacylglycerol (DAG) and IP_3, which activate protein kinase C and mobilize intracellular Ca^{2+} stores, respectively. It also serves as the substrate for PI 3-kinases and thus represents the precursor to PtdIns(3,4,5)P_3, which is an important second messenger in signal transduction. The major producers of PtdIns(4,5)P_2 are the PIPKIs, which must synthesize discrete pools of PtdIns(4,5)P_2 in a spatiotemporally-regulated manner to allow specific functions of PtdIns(4,5)P_2 to be executed.

To elucidate the *in vivo* role of specific PtdIns(4,5)P_2 pools we report the analysis of two mice: one harbouring a deletion of all splice isoforms of PIPKIγ (PIPKIγ$^{-/-}$), and one carrying a specific deletion of the PIPKIγ_i2 splice isoform (PIPKIγΔE17). We report that the PIPKIγΔE17 mouse has no significant aberrant phenotype, although fibroblasts and T cells lacking PIPKIγ_i2 display adhesion-related defects (Legate et al., 2011; Wernimont et al., 2010). It should be noted that the magnitude of the defects measured *in vitro* is small and does not appear to be important for normal development or physiological functioning, but the contribution of the PIPKIγ_i2-specific pool in challenge scenarios *in vivo* is so far untested. The PIPKIγ$^{-/-}$ mice experience perinatal death, in agreement with one of the two published models (Di Paolo et al., 2004). To establish a likely cause for the mortality in PIPKIγ$^{-/-}$ mice, we focused our analysis on three proposed functions for PIPKIγ: clathrin-mediated endocytosis, basolateral trafficking of E-cadherin in epithelia, and agonist-induced intracellular Ca^{2+} release. In so doing we establish that PIPKIγ_i2 is specifically required for

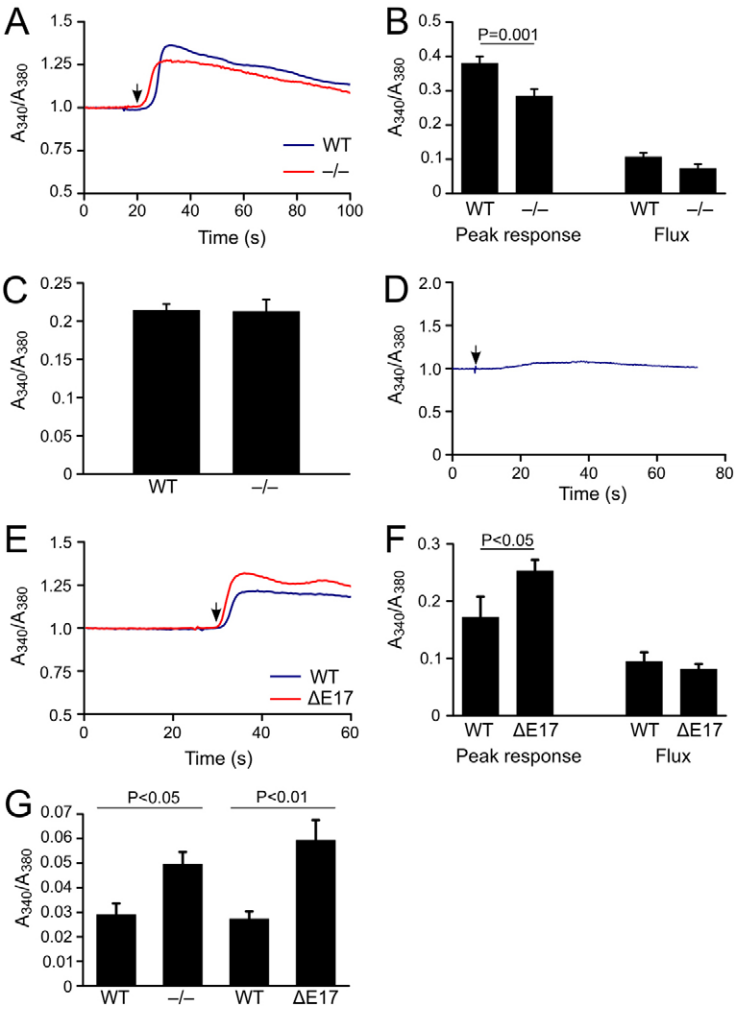

Fig. 5. Analysis of Ca^{2+} signaling. (**A**) Fura-2 ratiometric response of WT (blue line) and PIPKIγ$^{-/-}$ (red line) fibroblasts exposed to 100 μM ATP. Arrow indicates addition of ATP. (**B**) Peak ratiometric response and Ca^{2+} flux for 33 WT and 36 PIPKIγ$^{-/-}$ cells. (**C**) Peak ratiometric response for 16 WT and 12 PIPKIγ$^{-/-}$ fibroblasts exposed to 100 μM ATP in the presence of thapsigargin (5 μM). (**D**) Representative ratiometric response of fibroblasts exposed to 100 μM ATP in the presence of the PKC inhibitor U-73122 (20 μM). Arrow indicates addition of ATP. (**E**) Fura-2 ratiometric response of WT (blue line) and PIPKIγΔE17 (red line) fibroblasts exposed to 100 μM ATP. Arrow indicates addition of ATP. (**F**) Peak ratiometric response and Ca^{2+} flux for 21 WT and 23 PIPKIγΔE17 cells. (**G**) Peak ratiometric response of fibroblasts exposed to 1 mM extracellular Ca^{2+}. *N*=45 WT, 37 ΔE17; 21 WT, 20 $^{-/-}$. Data in B,C,F,G are mean±s.e.m.

endocytosis in neurons, PIPKIγ_i1 has a role in Ca^{2+} signaling in several cell types, and neither isoform is required for epithelial integrity.

The involvement of PIPKIγ in clathrin-mediated endocytosis at the synaptic membrane has been demonstrated using knockdown and overexpression approaches (Krauss et al., 2003; Nakano-Kobayashi et al., 2007) and through genetic disruption of all PIPKIγ isoforms (Di Paolo et al., 2004). PIPKIγ_i2 was shown to be the relevant splice isoform in neurons (Nakano-Kobayashi et al., 2007) and was also shown to be an important mediator of endocytosis in MDCK and HeLa cells (Bairstow et al., 2006). Mutational and structural analysis indicates that the 26 amino acid extension of PIPKIγ_i2 binds to the μ2 subunit of the AP-2 adaptor complex (Bairstow et al., 2006; Kahlfeldt et al., 2010), as well as to the β2 subunit (Nakano-Kobayashi et al., 2007; Thieman et al., 2009; Kahlfeldt et al., 2010), thereby localizing PIPKIγ_i2 to clathrin-coated pits. However, the kinase core domain of all PIPKIs also binds to μ2, raising the possibility that other PIPKIs and splice isoforms of PIPKIγ may stimulate endocytosis in some cell types (Krauss et al., 2006). By specifically ablating PIPKIγ_i2 throughout the whole mouse we provide direct proof that this isoform is the relevant splice isoform mediating endocytosis in neurons by using an established method to measure relative amounts of internalized synaptic vesicles (Gaffield and Betz, 2007). Both PIPKIγΔE17 and PIPKIγ$^{-/-}$ neurons had a comparable SV endocytosis defect, despite abundant levels of PIPKIγ_i1 in synaptosome fractions. However, PIPKIγ appears to play no role in endocytosis in both fibroblasts and splenic metallophilic macrophages. The main difference between these experiments is that SV endocytosis was induced by first depolarizing the neuron, whereas fibroblast and macrophage experiments measured constitutive endocytosis, which appears to require PIPKIα rather than PIPKIγ (Padrón et al., 2003). It is surprising that a ~50% reduction in synaptic vesicle endocytosis appears to have little effect on performance during a battery of behavioral and learning and memory tests aside from a reduction in the magnitude of the startle response in PIPKIγΔE17 mice. Although involuntary movement by PIPKIγΔE17 mice is reduced in this assay, the degree of inhibition by a prepulse stimulus is not changed indicating that hearing itself is not affected. Reduction of the acoustic startle response without affecting its prepulse inhibition has been observed previously, e.g. in parkin-deficient mice, which is thought to result from a reduction of norepinephrine (Von Coelln et al., 2004). Interference with noradrenergic neurotransmission by lesions or pharmacologically modulates the amplitude of the startle response. Reduction in synaptic vesicle recycling may very subtly affect, potentially circuit specific, the neurotransmitter balance or release, and thereby exert subtle effects on specific

behaviors. The reduction of brain PtdIns(4,5)P_2 content was previously proposed to be the cause of perinatal lethality in PIPKIγ$^{-/-}$ mice (Di Paolo et al., 2004). We show here that, of the potential roles of PIPKIγ-derived PtdIns(4,5)P_2 in brain function, the role in synaptic vesicle endocytosis is dispensable for life.

The most striking feature of newborn PIPKIγ$^{-/-}$ mice is an inability to feed. Since PIPKIγ contributes to the formation of cell-cell junctions though regulating trafficking of E- and N-cadherin (El Sayegh et al., 2007; Ling et al., 2007), we hypothesized that the failure to feed could be a consequence of disturbed epithelial integrity. Although biochemical data indicates that PIPKIγ_i2 is the most likely isoform to mediate cadherin trafficking (Ling et al., 2007), the localization of PIPKIγ_i1 to cell-cell junctions in A431 cells (Akiyama et al., 2005) and an interaction with the exocyst to mediate E-cadherin clustering (Xiong et al., 2012) suggests that this isoform may also play a role in the maintenance of cell-cell junctions. However, our analysis indicates that AJs form correctly in the mouse in the absence of PIPKIγ, and no obvious defects in either stratified or simple epithelium are observed. Also, the failure to identify PIPKIγ in cell-cell junctions of keratinocytes indicates that it is unlikely that PIPKIγ plays a role in the maintenance of the AJs of the skin, consistent with normal barrier formation in PIPKIγ$^{-/-}$ embryos and the lack of functional defects in PIPKIγ fl/fl$^{K5\text{-}Cre}$ mice. Our antibody did not work in tissue sections, so we were unable to test whether PIPKIγ localizes to AJs in kidney or gut epithelium, but the lack of histological abnormalities on the microscopic level suggest that AJs were fully able to form and be maintained in these tissues in the absence of PIPKIγ.

Increases in intracellular Ca^{2+} concentration occur in response to a variety of agonists via G protein-mediated phospholipase C (PLC) activation (Berridge, 2009). PLC cleaves PtdIns(4,5)P_2 into DAG and IP_3; the latter binds to receptors on the endoplasmic reticulum and stimulates the release of Ca^{2+} (Berridge, 2009). Knockdown or genetic ablation of PIPKIγ results in diminished intracellular [Ca^{2+}] changes in HeLa cells, mast cells and mesenchymal stem cells (Wang et al., 2004; Vasudevan et al., 2009; Yu et al., 2011), implicating PIPKIγ as the source of this pool of PtdIns(4,5)P_2. Cationic amino acid transporter (CAT-2) knockout mice provide indirect *in vivo* evidence for PIPKIγ involvement in Ca^{2+} signaling in smooth muscle (Chen et al., 2007). Tracheal rings from CAT-2$^{-/-}$ mice show reduced smooth muscle contraction in response to carbachol treatment, which correlates with a reduced expression level of PIPKIγ compared to WT. Exogenous introduction of the polycation spermine restored PIPKIγ levels through an undetermined mechanism, and restoration of PIPKIγ expression likewise restored tracheal ring contractility. Although Ca^{2+} levels were not measured in these samples, smooth muscle contraction is activated by Ca^{2+} signaling cascades that culminate in myosin light chain phosphorylation (Berridge, 2008; Takashima, 2009).

We found that fibroblasts, glial cells and smooth muscle cells from PIPKIγ$^{-/-}$ mice showed reduced intracellular Ca^{2+} release in response to metabotropic agonists (ATP and carbachol), in contrast to cells from PIPKIγΔE17 mice, which responded as WT. PIPKIγ$^{-/-}$ fibroblasts showed an increase in extracellular Ca^{2+} entry, in agreement with data from mast cells demonstrating that PIPKIγ inhibits the interaction of STIM1 and Orai1, thus impairing store-operated Ca^{2+} entry (SOCE) (Calloway et al., 2011). It is therefore interesting that PIPKIγΔE17 fibroblasts also show increased Ca^{2+} entry, despite the continued presence of PIPKIγ_i1. These data suggest that, in fibroblasts, PtdIns(4,5)P_2 synthesized by PIPKIγ_i1 does not inhibit SOCE, but rather the inhibitory PtdIns(4,5)P_2 may originate from PIPKIγ_i2. Therefore, both isoforms may play a role in Ca^{2+} signaling, with PIPKIγ_i1 providing the PtdIns(4,5)P_2 for IP_3-mediated release of internal Ca^{2+} stores, and PIPKIγ_i2 providing the PtdIns(4,5)P_2 to limit the extent of SOCE.

Of the three pathways studied, Ca^{2+} signaling was the only pathway that differed significantly between PIPKIγΔE17 and PIPKIγ$^{-/-}$ mice, and therefore presents a plausible reason for why PIPKIγ$^{-/-}$ mice die perinatally whereas PIPKIγΔE17 have a normal life span. Given the importance of Ca^{2+} signaling in a wide range of cellular functions, it is not possible at this time to definitively establish a single cause for PIPKIγ$^{-/-}$ lethality; conditional knockouts will give further insight. However, given the appearance of the mice at birth, and the fact that they survive for several hours, we propose two possibilities.

As previously noted, PIPKIγ$^{-/-}$ mice have impaired motility and an absence of milk in their stomachs (Di Paolo et al., 2004). While we attribute their sluggish behavior to dehydration and a lack of nutrition, there may be a molecular cause. Intracellular Ca^{2+} signaling regulates a wide array of neuronal processes (Berridge, 1998). Of particular note is the role of Ca^{2+} in Purkinje neurons, where IP_3-mediated Ca^{2+} release from the ER plays a role in long term depression, facilitating motor memory and coordination (Goto and Mikoshiba, 2011). Genetic ablation of other members of the intracellular Ca^{2+} release signaling pathway; glutamate receptor mGluR1 (Alba et al., 1994; Conquet et al., 1994), $G\alpha_q$ (Offermanns et al., 1997; Hartmann et al., 2004), PLCβ4 (Kim et al., 1997) and IP_3 receptor type 1 (Matsumoto et al., 1996) all result in ataxia and, in some cases, tremors and seizures. Although most mice had reduced viability, death often occurred after 3 weeks postnatally. Therefore, the early post-natal lethality of PIPKIγ$^{-/-}$ mice must arise from additional defects.

The inability to feed could also arise from defects within the gastrointestinal system. Coordinated peristalsis of the gastrointestinal tract is controlled by Ca^{2+} signaling through pacemaker cells called interstitial cells of Cajal (ICC) (Takaki, 2003). Although mice lacking ICC are able to swallow and obtain nutrition (Ward et al., 1994), postnatal blockade of ICC function results in profound cessation of peristalsis (Maeda et al., 1992), suggesting developmental compensation in the mice lacking ICC. Since a role for ICC in peristalsis appears to begin around birth (Roberts et al., 2010), impaired pacemaker function of ICC is unlikely to be developmentally compensated in our mice. Therefore, combined dysfunctional Ca^{2+} signaling in ICC and esophageal smooth muscle may collaborate to abolish peristaltic waves necessary for swallowing.

We have generated and analyzed two mice carrying genetic mutations at the PIPKIγ locus. One mouse lacks all isoforms of PIPKIγ whereas the other mouse carries a specific deletion of the PIPKIγ_i2 splice isoform. By introducing a third PIPKIγ$^{-/-}$ mouse to the already published models (Di Paolo et al., 2004; Wang et al., 2007) we corroborate one of these models and confirm that PIPKIγ$^{-/-}$ mice develop normally but die shortly after birth. By comparing our two models we confirm a neuron-specific endocytosis defect in PIPKIγ$^{-/-}$ mice, but rule out that this defect is lethal. Rather, the intracellular Ca^{2+} response to metabotropic agents differs markedly between PIPKIγ$^{-/-}$ and PIPKIγΔE17 mice, and may represent an essential function of

PIPKIγ. The mice we have examined here harbour the genetic mutation in all tissues, but the fact that our strategy was designed to allow for ablation in specific tissues using Cre-lox technology will permit future analysis using restricted Cre expression lines to further isolate the essential role of PIPKIγ.

Materials and Methods

Generation of knockout mice

Generation of PIPKIγΔE17 mice was previously described (Legate et al., 2011). To generate PIPKIγ$^{-/-}$ mice, a loxP site and Neo cassette flanked by frt sites was inserted into an ApaI site located between exon 17 and exon 18. A second loxP site was inserted at the PmlI site 2.3 kb into exon 18. A 7 kb 5′ recombination arm spanning a ClaI site upstream of exon 17 and the ApaI site downstream of exon 17, and a 2.3 kb 3′ recombination arm spanning PmlI and *Eco*RI sites downstream of exon 18, were used to recombine the targeting vector into the genome of 129 ES cells. Clones were screened by Southern blot by digesting with *Eco*RI and using a 476 bp probe spanning exon 7. Mouse genotyping was accomplished by PCR analysis of tail clips using 5′-TACTAACTGCTTCCCGCTGCTG-3′ (forward) and 5′-GTTTTCTGTGTCTTGTCGTC-3′ (reverse) to distinguish WT from ΔE17, and the WT allele of PIPKIγ$^{+/-}$ mice, and 5′-TACTAACTGCTTCCCGCTGCTG-3′ (forward) and 5′-AGTCATCTGCGAATTGGGATT-3′ to detect the null allele. The Neo cassette was removed by mating mice with a strain expressing a deletor flipase, and all mice were backcrossed for seven generations with CL57Bl/6 before analysis. WT littermates were used as controls against ΔE17 and −/− mice. All animal studies were approved by the Regierung von Oberbayern.

RT-PCR

RNA was isolated from tissues of 4-week-old mice using Trizol (Invitrogen) according to the manufacturer's directions. 1 µg of total RNA was reverse transcribed using a ProtoScript cDNA synthesis kit (NEB) using oligo d(T)$_{23}$ VN primers according to the manufacturer's directions. The single strand DNA was used as a template for a PCR reaction to detect the following transcripts: PIPKIα: 5′-GCAGAGAATCCAGACACAATG-3′ (forward), 5′-CTGATGGAGGATACG-ATCTC-3′ (reverse); PIPKIβ: 5′-TACAGGTTTGTTAAGAAGTTGG-3′ (forward), 5′-CTCTGCAACATCAAGCTTTTCC-3′ (reverse); PIPKIγ: 5′-CTTCAGATAC-ATCGGAGCAG-3′ (forward), 5′-GCTGGGCTCCAGATTGGGG-3′ (reverse); PIPKIγ_i2: 5′-CTTCAGATACATCGGAGCAG-3′ (forward), 5′-CGCTCTCGCC-GTCGGAGG-3′ (reverse); GAPDH: 5′-ACCACAGTCCATGCCATCAC-3′ (forward), 5′-TCCACCACCCTGTTGCTGTA-3′ (reverse).

Behavioral tests

The following behavioral tests were performed in sequential order: general neurological examination, grip strength, rotarod, open field, elevated-plus maze, light-dark avoidance, Morris water maze, shuttle box, and startle/prepulse inhibition as described previously (Montag-Sallaz et al., 2002; Montag-Sallaz and Montag, 2003; Beglopoulos et al., 2005).

Cell type isolation

Neurons were isolated from E14.5 embryos as described (Vincent et al., 1996). Briefly, cortices were dissected and mechanically dissociated with a flame polished pipette in Ham's F12 medium supplemented with 10% FBS and 0.6% glucose. Dissociated cells were plated at 3×10^6 cells/35 mm plastic cell culture dish coated with 10 µg/ml poly-L-lysine. After 3 days, 5 µM arabinofuranoside was added to the culture medium to prevent the proliferation of glial cells. Neurons were cultured for 10 days before experiments.

Fibroblasts were isolated as previously described (Legate et al., 2011), and keratinocytes were isolated as previously described (Czuchra et al., 2006).

Macrophages were isolated by negative magnetic selection. Spleens from 12-week old mice were rinsed in HBSS+0.2% BSA and separated into a single cell suspension by rubbing between two frosted glass slides and washed though a 70 µm cell strainer. Red blood cells were removed by incubation for 3 minutes in ACK buffer (150 mM NH_4Cl, 10 mM $KHCO_3$, 0.1 mM EDTA), HBSS was added to fill the tube and cell suspensions were pelleted at 900 rpm for 10 minutes. Pellets were resuspended in 5 ml MACS buffer (PBS +2 mM EDTA +0.5% BSA) and incubated with biotinylated antibodies against CD90, B220, Gr-1, NK1.1 (PharMingen) and DX5 (BD Biosciences) for 10 minutes on ice. Cells were washed, incubated with 100 µl streptavidin-MicroBeads (Miltenyi Biotec) for 15 minutes on ice, and applied to a MACS LS separation column (Miltenyi Biotec) in the presence of a magnetic field. The flow-through contained macrophages. Purity was controlled by staining with anti-F4/80-Alexa 647 and analyzed by FACS.

Glial cells were isolated from newborn cerebral cortices by gentle trituration with a pipette tip in Spinner MEM (SMEM). Cell suspensions were incubated with 2 mg/ml trypsin, 1 mM EDTA and 200 U/ml DNase (Sigma #D5025) in SMEM for 10 min at 37℃, and triturated again. Trypsin was killed by addition of an equal volume of DMEM +10% FBS and centrifuged. Pellets were resuspended in DMEM +10% FBS +Pen/Strep and plated at 1 brain per 2×10 cm dishes. Plates were split three times before experiments, and cell identity was confirmed by immunostaining with anti-GFAP antibody.

Smooth muscle cells were isolated from bladders of newborn mice. Bladders were dissected, washed in HBSS and rubbed with forceps to dissociate epithelial cells. Tissue was macerated and incubated for 1 hour at 37℃ in DMEM +2 mg/ml collagenase Type 2 (Worthington). Cell pellets were resuspended in DMEM +10% FBS +Pen/Strep and plated onto glass bottom 35 mm dishes coated with 10 µg/ml fibronectin, 3 dishes per bladder. Cells were used for experiments the next day. Identity of the cell type was confirmed by immunostaining with anti-smooth muscle actin.

Endocytosis assays

Neurons from E14.5 embryos were cultured in neural-basal medium containing B27 supplement and 5% FBS for 10 days before the experiments. Neurons were surface-labeled with 0.13 mg/ml NHS-SS-biotin (Thermo Scientific) for 30 minutes at 4℃ before incubation for 90 seconds in neural-basal medium containing 90 mM KCl. Endocytosis was induced by incubating the neurons in medium containing 4 mM KCl for 10 minutes at 37℃. The remaining surface label was stripped with sodium 2-mercaptoethanesulfonate (MesNa, Sigma) for 25 minutes at 4℃ before cells were lysed in a low volume of lysis buffer (75 mM Tris, 200 mM NaCl, 7.5 mM EDTA and 7.5 mM EGTA, 1.5% Triton X-100, 0.75% Igepal CA-630, and protease inhibitors). Biotinylated synaptotagmin was determined by Capture-ELISA. For this, 50 µl cell lysate was incubated overnight at 4℃ in Maxisorb 96 well plates (Life Technologies) that were coated overnight with anti-synaptotagmin antibody (5 µg/ml, Ab51172, Abcam) to capture synaptotagmin. Biotinylated synaptotagmin was detected after several washing steps by chromogenic reaction with ABTS peroxidase substrate (Vector Laboratories).

Alternately, neurons were loaded with 10 µM FM 4–64 in endocytosis buffer (10 mM HEPES, 130 mM NaCl, 1 mM $MgCl_2$, 30 mM glucose, pH 7.4) containing 90 mM KCl and 2 mM $CaCl_2$ for 2 minutes, followed by an incubation with 10 µM FM 4–64 in endocytosis buffer containing 4 mM KCl and 2 mM $CaCl_2$ for 10 minutes. To remove non-internalized dye, neurons were washed with 1 mM ADVASEP-7 (Biotrend) in endocytosis buffer containing 4 mM KCl and no $CaCl_2$ for 3×3 minutes. Images were collected in an environmental chamber maintained at 37℃ with a 20× 1.6 objective of a Zeiss Axiovert 200 M controlled by Metamorph software. Neurons were unloaded by 2×2 minute incubations in endocytosis buffer containing 90 mM KCl and 2 mM $CaCl_2$, and imaged again for background subtraction. Background subtracted images were generated in ImageJ, regions of interest were drawn around fluorescent synaptic boutons and integrated fluorescence intensity was quantified.

1.5×10^5 fibroblasts were plated into 6 cm dishes the day before the assay. Cells were incubated with 5 µg/ml transferrin-Alexa 488 (Invitrogen) in DMEM/0.1% BSA and incubated for 20 minutes at 37℃ (control samples were kept on ice during the incubation). Cells were washed 3× with PBS and incubated for 5 minutes in 0.5 M HOAc/0.5 M NaCl, pH 4.1 to remove non-internalized transferrin. Cells were washed again with PBS, scraped into tubes and centrifuged, resuspended in PBS/2% FBS and fixed with 1.5% PFA for 10 minutes prior to FACS analysis. 50,000 cells were counted per plot.

Isolated macrophages were resuspended in 100 µl MACS buffer containing 10 µg/ml transferrin-Alexa 488 and incubated for 15 minutes at 37℃. An excess of ice cold 0.5 M HOAc/0.5 M NaCl, pH 4.1 was added to the tubes and incubated for 5 minutes to remove non-internalized transferrin. Cells were washed twice with MACS buffer, labeled with anti-F4/80-Alexa 647 and analyzed by FACS. F4/80-positive cells were gated to remove minor F4/80-negative contamination from the analysis.

Synaptosome preparation

Crude synaptosomes were prepared by differential centrifugation as described (Huttner et al., 1983) and further fractionated on a discontinuous Ficoll gradient (Nicholls, 1978).

Tissue iron determination

Colorimetric quantification of tissue iron stores was a combination of two previously described methods (van Elik et al., 1974; Kreeftenberg et al., 1984). Liver and spleen samples were dissected, rinsed in 150 mM NaCl, and weighed prior to drying at 110℃. 200 µl of destruction fluid (perchloric acid:nitric acid 4:1 v/v) was added and samples were incubated for 3 hours at 60℃. Water was added to 3 ml, and 1 ml was withdrawn for analysis. 0.1 ml 0.1 M HCl, 0.1 ml 10 mM $K_2S_2O_8$ and 0.5 ml 5 M KCNS were added to obtain Fe-CNS complexes, which were extracted with two additions of methyl isobutyl ketone. Absorbance was read at 500 nm and compared to a standard $FeCl_3$ solution.

Histology and immunohistochemistry

Formalin fixed, paraffin-embedded spleens were sectioned into 5 µm thick slices with a microtome. To visualize iron content, spleen sections were deparaffinized, rehydrated, and incubated with a mixture of equal proportions 20% aqueous HCl

and 10% aqueous solution potassium ferrocyanide [$K_4Fe(CN)_6.3H_2O$] for 20 minutes, rinsed with dH_2O and counterstained with H&E. To visualize adherens junctions in epithelia skin, esophagus, small intestine and kidney samples were frozen and sectioned into 5 μm slices with a cryotome. Sections were fixed with 4% PFA, permeabilized with PBS/0.2% Triton X-100 for 10 minutes and incubated overnight with rat anti-E-cadherin (1:200; Zymed) and rabbit anti-laminin 332 (skin and esophagus; 1:1000; gift from Monique Aumailley) or rat anti-α6 integrin-FITC (kidney; 1:100; PharMingen); the latter incubation was conducted after secondary labeling of the E-cadherin was complete. Secondary antibodies were anti-rat-Cy3 (1:800; Jackson) and anti-rabbit-Alexa647 (1:500; Invitrogen).

Barrier function assays

Inside-out barrier function was assayed using a surface biotinylation technique as described (Furuse et al., 2002). 50 μl of a 10 mg/ml solution of EZ-Link Sulfo-NHS-LC-Biotin (Pierce) resuspended in PBS +1 mM $CaCl_2$ was injected into the back skin of WT or PIPKI$\gamma^{-/-}$ newborn mice and incubated for 30 minutes. Skin samples were frozen, sectioned at 5 μm thickness, fixed in 95% ethanol for 30 minutes at 4℃ and 100% acetone for 1 minute at room temp. Samples were blocked for 15 minutes and incubated with Streptavidin-Cy3 (source) for 30 minutes.

Outside-in barrier function was analyzed by a whole-mount permeability assay as previously described (Hardman et al., 1998). Embryos were incubated with 4 mM $K_4Fe(CN)_6.3H_2O$, 4 mM $K_3Fe(CN)_6$, 1 mg/ml 5-bromo-4-chloro-3-indolyl-β, D-galactopyranoside (X-Gal) in PBS, pH 4.5 at 30℃ overnight, and photographed.

Calcium release assay

Cells plated on glass bottom 35 mm dishes were loaded with 4 μM Fura-2, AM (Invitrogen) for 1 hour at room temp in loading buffer (110 mM HEPES-NaOH, 135 mM NaCl, 5 mM KCl, 1 mM $MgCl_2$, 3 mM $CaCl_2$, 25 mM glucose, pH 7.4) and incubated a further 30 minutes in wash/assay buffer (loading buffer, $CaCl_2$) to allow the Fura-2 to de-esterify (SMCs were incubated during this step in load buffer since prolonged incubation in calcium-free buffer resulted in a lack of response to agonist). Cells were imaged on a Zeiss Axiovert 35 M microscope equipped with a CoolSnap charge-coupled device camera. Imaging and data collection was controlled by Metafluor version 4.6 software. For ratiometric imaging 320 and 360 excitation filters and a 500/20 emission filter were used. Immediately prior to imaging, the buffer bathing the SMCs was exchanged for calcium-free assay buffer. Baseline ratios were collected every 3 seconds (for glia and SMCs, every 0.5 seconds for fibroblasts) for 1 minute. Agonists used were 100 μM ATP for fibroblasts and glia and 100 μM carbamoylcholine chloride (Cch; Sigma) for SMCs. Following the addition of agonist, ratios were collected for an additional 4–9 minutes. Peak responses were calculated as the difference between the baseline values and maximal ratiometric change, and flux was measured by calculating the slope of the ratiometric change (Fura-2 ratio over time) during the linear portion of the cellular response.

Statistical analysis

Where stated, results are expressed as means±s.e.m. Unpaired Student's *t*-test was used to establish statistical significance. For behavioral experiments analysis of variance (ANOVA) with factors genotype and sex and post hoc analysis with Scheffe's was used.

Acknowledgements

The authors would like to thank K. Sowa and A. Reichel for excellent technical assistance for the behavioural experiments, F. Swirski for advice on macrophage isolation, and K. Scheidt and J. Mackinnon for assistance with Ca^{2+} measurements.

Funding

This work was supported by a Marie Curie fellowship under the European Community 6th framework program (to K.R.L.); the Deutsche Forschungsgemeinschaft (DFG) [grant number SFB 863 to R.F.]; and the Max Planck Society (to R.F.).

Supplementary material available online at
http://jcs.biologists.org/lookup/suppl/doi:10.1242/jcs.102145/-/DC1

References

Alba, A., Kano, M., Chen, C., Stanton, M. E., Fox, G. D., Herrup, K., Zwingman, T. A. and Tonegawa, S. (1994). Deficient cerebellar long-term depression and impaired motor learning in mGluR1 mutant mice. *Cell* **79**, 377-388.

Aikawa, Y. and Martin, T. F. J. (2003). ARF6 regulates a plasma membrane pool of phosphatidylinositol(4,5)bisphosphate required for regulated exocytosis. *J. Cell Biol.* **162**, 647-659.

Akiyama, C., Shinozaki-Narikawa, N., Kitazawa, T., Hamakubo, T., Kodama, T. and Shibasaki, Y. (2005). Phosphatidylinositol-4-phosphate 5-kinase gamma is associated with cell-cell junction in A431 epithelial cells. *Cell Biol. Int.* **29**, 514-520.

Bairstow, S. F., Ling, K., Su, X., Firestone, A. J., Carbonara, C. and Anderson, R. A. (2006). Type Igamma661 phosphatidylinositol phosphate kinase directly interacts with AP2 and regulates endocytosis. *J. Biol. Chem.* **281**, 20632-20642.

Beglopoulos, V., Montag-Sallaz, M., Rohlmann, A., Piechotta, K., Ahmad, M., Montag, D. and Missler, M. (2005). Neurexophilin 3 is highly localized in cortical and cerebellar regions and is functionally important for sensorimotor gating and motor coordination. *Mol. Cell. Biol.* **25**, 7278-7288.

Berridge, M. J. (1998). Neuronal calcium signaling. *Neuron* **21**, 13-26.

Berridge, M. J. (2008). Smooth muscle cell calcium activation mechanisms. *J. Physiol.* **586**, 5047-5061.

Berridge, M. J. (2009). Inositol trisphosphate and calcium signalling mechanisms. *Biochim. Biophys. Acta* **1793**, 933-940.

Calderwood, D. A., Tai, V., Di Paolo, G., De Camilli, P. and Ginsberg, M. H. (2004). Competition for talin results in trans-dominant inhibition of integrin activation. *J. Biol. Chem.* **279**, 28889-28895.

Calloway, N., Owens, T., Corwith, K., Rodgers, W., Holowka, D. and Baird, B. (2011). Stimulated association of STIM1 and Orai1 is regulated by the balance of PtdIns(4,5)P_2 between distinct membrane pools. *J. Cell Sci.* **124**, 2602-2610.

Chen, H., Macleod, C., Deng, B., Mason, L., Kasaian, M., Goldman, S., Wolf, S., Williams, C. and Bowman, M. R. (2007). CAT-2 amplifies the agonist-evoked force of airway smooth muscle by enhancing spermine-mediated phosphatidylinositol-(4)-phosphate-5-kinase-gamma activity. *Am. J. Physiol. Lung Cell Mol. Physiol.* **293**, L883-L891.

Conquet, F., Bashir, Z. I., Davies, C. H., Daniel, H., Ferraguti, F., Bordi, F., Franz-Bacon, K., Reggiani, A., Matarese, V., Condé, F. et al. (1994). Motor deficit and impairment of synaptic plasticity in mice lacking mGluR1. *Nature* **372**, 237-243.

Czuchra, A., Meyer, H., Legate, K. R., Brakebusch, C. and Fässler, R. (2006). Genetic analysis of beta1 integrin "activation motifs" in mice. *J. Cell Biol.* **174**, 889-899.

de Pereda, J. M., Wegener, K. L., Santelli, E., Bate, N., Ginsberg, M. H., Critchley, D. R., Campbell, I. D. and Liddington, R. C. (2005). Structural basis for phosphatidylinositol phosphate kinase type Igamma binding to talin at focal adhesions. *J. Biol. Chem.* **280**, 8381-8386.

Di Paolo, G., Pellegrini, L., Letinic, K., Cestra, G., Zoncu, R., Voronov, S., Chang, S., Guo, J., Wenk, M. R. and De Camilli, P. (2002). Recruitment and regulation of phosphatidylinositol phosphate kinase type 1 gamma by the FERM domain of talin. *Nature* **420**, 85-89.

Di Paolo, G., Moskowitz, H. S., Gipson, K., Wenk, M. R., Voronov, S., Obayashi, M., Flavell, R., Fitzsimonds, R. M., Ryan, T. A. and De Camilli, P. (2004). Impaired PtdIns(4,5)*P*2 synthesis in nerve terminals produces defects in synaptic vesicle trafficking. *Nature* **431**, 415-422.

Doughman, R. L., Firestone, A. J. and Anderson, R. A. (2003). Phosphatidylinositol phosphate kinases put PI4,5P(2) in its place. *J. Membr. Biol.* **194**, 77-89.

El Sayegh, T. Y., Arora, P. D., Ling, K., Laschinger, C., Janmey, P. A., Anderson, R. A. and McCulloch, C. A. (2007). Phosphatidylinositol-4,5 bisphosphate produced by PIP5KIgamma regulates gelsolin, actin assembly, and adhesion strength of N-cadherin junctions. *Mol. Biol. Cell* **18**, 3026-3038.

Furuse, M., Hata, M., Furuse, K., Yoshida, Y., Haratake, A., Sugitani, Y., Noda, T., Kubo, A. and Tsukita, S. (2002). Claudin-based tight junctions are crucial for the mammalian epidermal barrier: a lesson from claudin-1-deficient mice. *J. Cell Biol.* **156**, 1099-1111.

Gaffield, M. A. and Betz, W. J. (2007). Imaging synaptic vesicle exocytosis and endocytosis with FM dyes. *Nat. Protoc.* **1**, 2916-2921.

Giudici, M.-L., Emson, P. C. and Irvine, R. F. (2004). A novel neuronal-specific splice variant of Type I phosphatidylinositol 4-phosphate 5-kinase isoform gamma. *Biochem. J.* **379**, 489-496.

Giudici, M.-L., Lee, K., Lim, R. and Irvine, R. F. (2006). The intracellular localisation and mobility of Type Igamma phosphatidylinositol 4P 5-kinase splice variants. *FEBS Lett.* **580**, 6933-6937.

Gong, L.-W., Di Paolo, G., Diaz, E., Cestra, G., Diaz, M.-E., Lindau, M., De Camilli, P. and Toomre, D. (2005). Phosphatidylinositol phosphate kinase type I gamma regulates dynamics of large dense-core vesicle fusion. *Proc. Natl. Acad. Sci. USA* **102**, 5204-5209.

Goto, J.-I. and Mikoshiba, K. (2011). Inositol 1,4,5-trisphosphate receptor-mediated calcium release in purkinje cells: from molecular mechanism to behavior. *Cerebellum*, **10**, 820-833.

Hardman, M. J., Sisi, P., Banbury, D. N. and Byrne, C. (1998). Patterned acquisition of skin barrier function during development. *Development* **125**, 1541-1552.

Hartmann, J., Blum, R., Kovalchuk, Y., Adelsberger, H., Kuner, R., Durand, G. M., Miyata, M., Kano, M., Offermanns, S. and Konnerth, A. (2004). Distinct roles of Galpha(q) and Galpha11 for Purkinje cell signaling and motor behavior. *J. Neurosci.* **24**, 5119-5130.

Huttner, W. B., Schiebler, W., Greengard, P. and De Camilli, P. (1983). Synapsin I (protein I), a nerve terminal-specific phosphoprotein. III. Its association with synaptic vesicles studied in a highly purified synaptic vesicle preparation. *J. Cell Biol.* **96**, 1374-1388.

Ishihara, H., Shibasaki, Y., Kizuki, N., Katagiri, H., Yazaki, Y., Asano, T. and Oka, Y. (1996). Cloning of cDNAs encoding two isoforms of 68-kDa type I phosphatidylinositol-4-phosphate 5-kinase. *J. Biol. Chem.* **271**, 23611-23614.

Ishihara, H., Shibasaki, Y., Kizuki, N., Wada, T., Yazaki, Y., Asano, T. and Oka, Y. (1998). Type I phosphatidylinositol-4-phosphate 5-kinases. Cloning of the third isoform and deletion/substitution analysis of members of this novel lipid kinase family. *J. Biol. Chem.* **273**, 8741-8748.

Kahlfeldt, N., Vahedi-Faridi, A., Koo, S. J., Schäfer, J. G., Krainer, G., Keller, S., Saenger, W., Krauss, M. and Haucke, V. (2010). Molecular basis for association of PIPKI gamma-p90 with clathrin adaptor AP-2. *J. Biol. Chem.* **285**, 2734-2749.

Kim, D., Jun, K. S., Lee, S. B., Kang, N.-G., Min, D. S., Kim, Y.-H., Ryu, S. H., Suh, P.-G. and Shin, H.-S. (1997). Phospholipase C isozymes selectively couple to specific neurotransmitter receptors. *Nature* **389**, 290-293.

Krauss, M., Kinuta, M., Wenk, M. R., De Camilli, P., Takei, K. and Haucke, V. (2003). ARF6 stimulates clathrin/AP-2 recruitment to synaptic membranes by activating phosphatidylinositol phosphate kinase type Igamma. *J. Cell Biol.* **162**, 113-124.

Krauss, M., Kukhtina, V., Pechstein, A. and Haucke, V. (2006). Stimulation of phosphatidylinositol kinase type I-mediated phosphatidylinositol (4,5)-bisphosphate synthesis by AP-2mu-cargo complexes. *Proc. Natl. Acad. Sci. USA* **103**, 11934-11939.

Kreeftenberg, H. G., Koopman, B. J., Huizenga, J. R., van Vilsteren, T., Wolthers, B. G. and Gips, C. H. (1984). Measurement of iron in liver biopsies—a comparison of three analytical methods. *Clin. Chim. Acta* **144**, 255-262.

Legate, K. R., Takahashi, S., Bonakdar, N., Fabry, B., Boettiger, D., Zent, R. and Fässler, R. (2011). Integrin adhesion and force coupling are independently regulated by localized PtdIns(4,5)2 synthesis. *EMBO J.* **30**, 4539-4553.

Ling, K., Doughman, R. L., Firestone, A. J., Bunce, M. W. and Anderson, R. A. (2002). Type I gamma phosphatidylinositol phosphate kinase targets and regulates focal adhesions. *Nature* **420**, 89-93.

Ling, K., Bairstow, S. F., Carbonara, C., Turbin, D. A., Huntsman, D. G. and Anderson, R. A. (2007). Type I gamma phosphatidylinositol phosphate kinase modulates adherens junction and E-cadherin trafficking via a direct interaction with mu 1B adaptin. *J. Cell Biol.* **176**, 343-353.

Loijens, J. C. and Anderson, R. A. (1996). Type I phosphatidylinositol-4-phosphate 5-kinases are distinct members of this novel lipid kinase family. *J. Biol. Chem.* **271**, 32937-32943.

Lokuta, M. A., Senetar, M. A., Bennin, D. A., Nuzzi, P. A., Chan, K. T., Ott, V. L. and Huttenlocher, A. (2007). Type Igamma PIP kinase is a novel uropod component that regulates rear retraction during neutrophil chemotaxis. *Mol. Biol. Cell* **18**, 5069-5080.

Maeda, H., Yamagata, A., Nishikawa, S., Yoshinaga, K., Kobayashi, S., Nishi, K. and Nishikawa, S. (1992). Requirement of c-kit for development of intestinal pacemaker system. *Development* **116**, 369-375.

Mao, Y. S., Yamaga, M., Zhu, X., Wei, Y., Sun, H.-Q., Wang, J., Yun, M., Wang, Y., Di Paolo, G., Bennett, M. et al. (2009). Essential and unique roles of PIP5K-gamma and -alpha in Fcgamma receptor-mediated phagocytosis. *J. Cell Biol.* **184**, 281-296.

Matsumoto, M., Nakagawa, T., Inoue, T., Nagata, E., Tanaka, K., Takano, H., Minowa, O., Kuno, J., Sakakibara, S., Yamada, M. et al. (1996). Ataxia and epileptic seizures in mice lacking type 1 inositol 1,4,5-trisphosphate receptor. *Nature* **379**, 168-171.

Montag-Sallaz, M. and Montag, D. (2003). Severe cognitive and motor coordination deficits in tenascin-R-deficient mice. *Genes Brain Behav.* **2**, 20-31.

Montag-Sallaz, M., Schachner, M. and Montag, D. (2002). Misguided axonal projections, neural cell adhesion molecule 180 mRNA upregulation, and altered behavior in mice deficient for the close homolog of L1. *Mol. Cell. Biol.* **22**, 7967-7981.

Nakano-Kobayashi, A., Yamazaki, M., Unoki, T., Hongu, T., Murata, C., Taguchi, R., Katada, T., Frohman, M. A., Yokozeki, T. and Kanaho, Y. (2007). Role of activation of PIP5Kgamma661 by AP-2 complex in synaptic vesicle endocytosis. *EMBO J.* **26**, 1105-1116.

Nicholls, D. G. (1978). Calcium transport and porton electrochemical potential gradient in mitochondria from guinea-pig cerebral cortex and rat heart. *Biochem. J.* **170**, 511-522.

Offermanns, S., Hashimoto, K., Watanabe, M., Sun, W., Kurihara, H., Thompson, R. F., Inoue, Y., Kano, M. and Simon, M. I. (1997). Impaired motor coordination and persistent multiple climbing fiber innervation of cerebellar Purkinje cells in mice lacking Galphaq. *Proc. Natl. Acad. Sci. USA* **94**, 14089-14094.

Padrón, D., Wang, Y. J., Yamamoto, M., Yin, H. and Roth, M. G. (2003). Phosphatidylinositol phosphate 5-kinase Ibeta recruits AP-2 to the plasma membrane and regulates rates of constitutive endocytosis. *J. Cell Biol.* **162**, 693-701.

Powner, D. J., Payne, R. M., Pettitt, T. R., Giudici, M. L., Irvine, R. F. and Wakelam, M. J. O. (2005). Phospholipase D2 stimulates integrin-mediated adhesion via phosphatidylinositol 4-phosphate 5-kinase Igamma b. *J. Cell Sci.* **118**, 2975-2986.

Roberts, R. R., Ellis, M., Gwynne, R. M., Bergner, A. J., Lewis, M. D., Beckett, E. A., Bornstein, J. C. and Young, H. M. (2010). The first intestinal motility patterns in fetal mice are not mediated by neurons or interstitial cells of Cajal. *J. Physiol.* **588**, 1153-1169.

Sasaki, J., Sasaki, T., Yamazaki, M., Matsuoka, K., Taya, C., Shitara, H., Takasuga, S., Nishio, M., Mizuno, K., Wada, T. et al. (2005). Regulation of anaphylactic responses by phosphatidylinositol phosphate kinase type I alpha. *J. Exp. Med.* **201**, 859-870.

Schill, N. J. and Anderson, R. A. (2009). Two novel phosphatidylinositol-4-phosphate 5-kinase type Igamma splice variants expressed in human cells display distinctive cellular targeting. *Biochem. J.* **422**, 473-482.

Schramp, M., Thapa, N., Heck, J. and Anderson, R. (2011). PIPKIγ regulates β-catenin transcriptional activity downstream of growth factor receptor signaling. *Cancer Res.* **71**, 1282-1291.

Sun, Y., Ling, K., Wagoner, M. P. and Anderson, R. A. (2007). Type I gamma phosphatidylinositol phosphate kinase is required for EGF-stimulated directional cell migration. *J. Cell Biol.* **178**, 297-308.

Sun, Y., Turbin, D. A., Ling, K., Thapa, N., Leung, S., Huntsman, D. G. and Anderson, R. A. (2010). Type I gamma phosphatidylinositol phosphate kinase modulates invasion and proliferation and its expression correlates with poor prognosis in breast cancer. *Breast Cancer Res.* **12**, R6.

Takaki, M. (2003). Gut pacemaker cells: the interstitial cells of Cajal (ICC). *J. Smooth Muscle Res.* **39**, 137-161.

Takashima, S. (2009). Phosphorylation of myosin regulatory light chain by myosin light chain kinase, and muscle contraction. *Circ. J.* **73**, 208-213.

Thapa, N., Sun, Y., Schramp, M., Choi, S., Ling, K. and Anderson, R. A. (2012). Phosphoinositide signaling regulates the exocyst complex and polarized integrin trafficking in directionally migrating cells. *Dev. Cell* **22**, 116-130.

Thieman, J. R., Mishra, S. K., Ling, K., Doray, B., Anderson, R. A. and Traub, L. M. (2009). Clathrin regulates the association of PIPKIgamma661 with the AP-2 adaptor beta2 appendage. *J. Biol. Chem.* **284**, 13924-13939.

Tomas, A., Yermen, B., Regazzi, R., Pessin, J. E. and Halban, P. A. (2010). Regulation of insulin secretion by phosphatidylinositol-4,5-bisphosphate. *Traffic* **11**, 123-137.

Toyofuku, T., Yoshida, J., Sugimoto, T., Zhang, H., Kumanogoh, A., Hori, M. and Kikutani, H. (2005). FARP2 triggers signals for Sema3A-mediated axonal repulsion. *Nat. Neurosci.* **8**, 1712-1719.

van Elik, H. G., Wiltink, W. F., Bos, G. and Goossens, J. P. (1974). Measurement of the iron content in human liver specimens. *Clin. Chim. Acta* **50**, 275-280.

Vasudevan, L., Jeromin, A., Volpicelli-Daley, L., De Camilli, P., Holowka, D. and Baird, B. (2009). The beta- and gamma-isoforms of type I PIP5K regulate distinct stages of Ca2+ signaling in mast cells. *J. Cell Sci.* **122**, 2567-2574.

Vincent, B., Beaudet, A., Dauch, P., Vincent, J. P. and Checler, F. (1996). Distinct properties of neuronal and astrocytic endopeptidase 3.4.24.16: a study on differentiation, subcellular distribution, and secretion processes. *J. Neurosci.* **16**, 5049-5059.

Volpicelli-Daley, L. A., Lucast, L., Gong, L.-W., Liu, L., Sasaki, J., Sasaki, T., Abrams, C. S., Kanaho, Y. and De Camilli, P. (2010). Phosphatidylinositol-4-phosphate 5-kinases and phosphatidylinositol 4,5-bisphosphate synthesis in the brain. *J. Biol. Chem.* **285**, 28708-28714.

Von Coelln, R., Thomas, B., Savitt, J. M., Lim, K. L., Sasaki, M., Hess, E. J., Dawson, V. L. and Dawson, T. M. (2004). Loss of locus coeruleus neurons and reduced startle in parkin null mice. *Proc. Natl. Acad. Sci. USA* **101**, 10744-10749.

Wang, Y. J., Li, W. H., Wang, J., Xu, K., Dong, P., Luo, X. and Yin, H. L. (2004). Critical role of PIP5KIgamma87 in InsP3-mediated Ca(2+) signaling. *J. Cell Biol.* **167**, 1005-1010.

Wang, Y., Lian, L., Golden, J. A., Morrisey, E. E. and Abrams, C. S. (2007). PIP5KI gamma is required for cardiovascular and neuronal development. *Proc. Natl. Acad. Sci. USA* **104**, 11748-11753.

Wang, Y., Chen, X., Lian, L., Tang, T., Stalker, T. J., Sasaki, T., Kanaho, Y., Brass, L. F., Choi, J. K., Hartwig, J. H. et al. (2008a). Loss of PIP5KIbeta demonstrates that PIP5KI isoform-specific PIP2 synthesis is required for IP3 formation. *Proc. Natl. Acad. Sci. USA* **105**, 14064-14069.

Wang, Y., Litvinov, R. I., Chen, X., Bach, T. L., Lian, L., Petrich, B. G., Monkley, S. J., Kanaho, Y., Critchley, D. R., Sasaki, T. et al. (2008b). Loss of PIP5KIgamma, unlike other PIP5KI isoforms, impairs the integrity of the membrane cytoskeleton in murine megakaryocytes. *J. Clin. Invest.* **118**, 812-819.

Ward, S. M., Burns, A. J., Torihashi, S. and Sanders, K. M. (1994). Mutation of the proto-oncogene c-kit blocks development of interstitial cells and electrical rhythmicity in murine intestine. *J. Physiol.* **480**, 91-97.

Wenk, M. R., Pellegrini, L., Klenchin, V. A., Di Paolo, G., Chang, S., Daniell, L., Arioka, M., Martin, T. F. and De Camilli, P. (2001). PIP kinase Igamma is the major PI(4,5)*P*(2) synthesizing enzyme at the synapse. *Neuron* **32**, 79-88.

Wernimont, S. A., Legate, K. R., Simonson, W. T. N., Fässler, R. and Huttenlocher, A. (2010). PIPKI gamma 90 negatively regulates LFA-1-mediated adhesion and activation in antigen-induced CD4+ T cells. *J. Immunol.* **185**, 4714-4723.

Xia, Y., Irvine, R. F. and Giudici, M.-L. (2011). Phosphatidylinositol 4-phosphate 5-kinase Iγ_v6, a new splice variant found in rodents and humans. *Biochem. Biophys. Res. Commun.* **411**, 416-420.

Xiong, X., Xu, Q., Huang, Y., Singh, R. D., Anderson, R., Leof, E., Hu, J. and Ling, K. (2012). An association between type Iγ PI4P 5-kinase and Exo70 directs E-cadherin clustering and epithelial polarization. *Mol. Biol. Cell* **23**, 87-98.

Xu, W., Wang, P., Petri, B., Zhang, Y., Tang, W., Sun, L., Kress, H., Mann, T., Shi, Y., Kubes, P. et al. (2010). Integrin-induced PIP5K1C kinase polarization regulates neutrophil polarization, directionality, and in vivo infiltration. *Immunity* **33**, 340-350.

Yu, Y.-L., Chou, R.-H., Chen, L.-T., Shyu, W.-C., Hsieh, S.-C., Wu, C.-S., Zeng, H.-J., Yeh, S.-P., Yang, D.-M., Hung, S.-C. et al. (2011). EZH2 regulates neuronal differentiation of mesenchymal stem cells through PIP5K1C-dependent calcium signaling. *J. Biol. Chem.* **286**, 9657-9667.